

ACCEPTED VERSION

**Title: Accumulated Bending Energy Elicits Neutral Sphingomyelinase Activity in Human Red Blood Cells**

Authors: David J. López<sup>1</sup>, Meritxell Egido-Gabas<sup>2</sup>, Iván López-Montero<sup>3</sup>, Jon V. Busto<sup>1</sup>, Josefina Casas<sup>2</sup>, Marie Garnier<sup>4</sup>, Francisco Monroy<sup>3</sup>, Banafshé Larijani<sup>4</sup>, Félix M. Goñi<sup>1</sup>, Alicia Alonso<sup>1</sup>

<sup>1</sup>Unidad de Biofísica (Centro Mixto CSIC-UPV/EHU) and Departamento de Bioquímica, Universidad País Vasco, Spain

<sup>2</sup>Departament de Química Biomedica, Institut de Química Avançada de Catalunya (IQAC-CSIC), Barcelona, Spain

<sup>3</sup>Mechanics of Biological Membranes and Biorheology, Departamento de Química Física I, Universidad Complutense de Madrid, Madrid, Spain

<sup>4</sup>Cell Biophysics Laboratory, London Research Institute, Cancer Research UK, London, United Kingdom

## Abstract

We propose that accumulated membrane bending energy elicits a neutral sphingomyelinase (SMase) activity in human erythrocytes. Membrane bending was achieved by osmotic or chemical processes, and SMase activity was assessed by quantitative thin-layer chromatography, high-performance liquid chromatography, and electrospray ionization-mass spectrometry. The activity induced by hypotonic stress in erythrocyte membranes had the pH dependence, ion dependence, and inhibitor sensitivity of mammalian neutral SMases. The activity caused a decrease in SM contents, with a minimum at 6 min after onset of the hypotonic conditions, and then the SM contents were recovered. We also elicited SMase activity by adding lysophosphatidylcholine externally or by generating it with phospholipase A(2). The same effect was observed upon addition of chlorpromazine or sodium deoxycholate at concentrations below the critical micellar concentration, and even under hypertonic conditions. A unifying factor of the various agents that elicit this SMase activity is the accumulated membrane bending energy. Both hypo- and hypertonic conditions impose an increased curvature, whereas the addition of surfactants or phospholipase A(2) activation increases the outer monolayer area, thus leading to an increased bending energy. The fact that this latent SMase activity is tightly coupled to the membrane bending properties suggests that it may be related to the general phenomenon of stress-induced ceramide synthesis and apoptosis.

## Introduction

Membrane curvature is generated as a result of a complex interplay among membrane proteins, lipids, and physical forces that are applied to the membrane surface (1). Helfrich (2) introduced the concept of spontaneous curvature  $J_s$  as a physical factor characterizing the tendency of a flat membrane to bend. To change membrane curvature, forces have to be applied to the membrane and energy has to be invested. Membrane resistance to deviations of curvature from  $J_s$  is determined by the bending rigidity  $\kappa$ . The latter is determined mainly by the bilayer composition at a given temperature. According to the Helfrich bending model, the bending stress, or bending moment  $\tau$ , depends on the rigidity and the difference between the imposed and the spontaneous curvature:

$$(1) \quad \tau = k(J - J_s).$$

As described in Eq. 1, in terms of the Helfrich bending model (2), the bending stress is related to the difference between the actual and the spontaneous curvature ( $J - J_s$ ). The accumulated bending energy per unit area ( $f_B$ ) required to deform a monolayer from its spontaneous curvature  $J_s$  to a mean curvature  $J$  is given by

$$(2) \quad f_B = \frac{1}{2}k(J - J_s)^2.$$

For years, sphingolipids have been considered as mere structural lipids in cells; however, over the past decade their role in cell signaling has been highlighted. A particularly well studied sphingolipid is ceramide, which acts as an important second messenger in cell death processes (3). It has also been described as having a putative role as an inducer of cell proliferation (4). Ceramide may be synthesized via two different pathways: de novo synthesis or sphingomyelin (SM) hydrolysis. The first one occurs in the endoplasmic reticulum (5) via condensation of L-serine with palmitoyl-CoA to form 3-ketosphinganine. The second pathway appears to occur mainly in the plasma membrane, as a result of sphingomyelinase (SMase) activation by an appropriate effector of the sphingolipid signaling pathway (6).

Lang et al. (7), investigating the processes that occur during erythrocyte death, described an increase in ceramide content after a 15-h incubation of human red blood cells (RBCs) in a hypertonic medium. Other authors (8, 9) had reported some years previously that incubation of chicken erythrocytes in a hypotonic medium resulted in the hydrolysis of SM. Because of the newly acknowledged importance of ceramide signaling in RBCs as well as in other cells, it was important to explore and define any latent SMase activity in human erythrocytes. This work deals with the characterization of a SMase activity in human RBCs that is elicited upon an increase in the membrane bending energy. We monitored the bending-energy-dependent decrease in SM content by using three different techniques, namely, thin-layer chromatography (TLC), reverse-phase high-performance liquid chromatography (RP-HPLC), and

electrospray ionization mass spectrometry (ESI-MS). Up to seven different groups of SMases have been described (10). Some of those that are present in mammals are active at neutral pH only in the presence of magnesium ions. One type of neutral SMase, nSMase-2 (11), has been localized in the plasma membrane, is magnesium-dependent, and is inhibited by nSMase inhibitors such as GW4869. The activity described in this work may belong to this group of neutral SMases.

## Materials and Methods

### Materials

Silica G-60 plates and solvents for chromatographic assays were obtained from Merck (Darmstadt, Germany). *N*-2-hydroxyethylpiperazine-*N'*-2-ethanesulfonic acid (HEPES) was purchased from Apollo Scientific Ltd. (Cheshire, UK). Trypsin,  $\alpha$ -chymotrypsin, chlorpromazine (CPZ), phospholipase A<sub>2</sub> (PLA<sub>2</sub>) from hog pancreas, GW4869, and detergents were obtained from Sigma Aldrich (St. Louis, MO). Spiroepoxide was purchased from Alexis (San Diego, CA). *N*-(4,4-difluoro-5,7-dimethyl-4-bora-3a,4a-diaza-s-indacene-3-dodecanoyl)sphingosylphosphocholine (BODIPY-C<sub>12</sub>-SM) and 6-((*N*-(7-nitrobenz-2-oxa-1,3-diazol-4-yl)amino)hexanoyl)sphingosylphosphocholine (NBD-C<sub>6</sub>-SM) were obtained from Molecular Probes (Eugene, OR). 6-((*N*-(7-nitrobenz-2-oxa-1,3-diazol-4-yl)amino)hexanoyl)sphingosine (NBD-C<sub>6</sub>-ceramide) was synthesized according to Bedia et al. (12). Mass spectrometry standards 1,2-dilauroyl-*sn*-glycero-3-phosphocholine (DLPC), 1,2-dilauroyl-*sn*-glycero-3-phosphoethanolamine (DLPE), 1,2-dilauroyl-*sn*-glycero-3-[phospho-L-serine] (DLPS), 1,2-dilauroyl-*sn*-glycero-3-phosphate (DLPA), and 1,2-dilauroyl-*sn*-glycero-3-[phospho-rac-(1-glycerol)] (DLPG) were purchased from Avanti Polar Lipids (Alabaster, AL), and 1,2-dipalmitoyl-*sn*-glycero-3-phosphatidylinositol (DPPI) was obtained from Echelon (Salt Lake City, UT).

### Blood sample preparation

Blood was withdrawn from healthy donors and washed three times in buffer A (isotonic) containing 32 mM HEPES, 125 mM NaCl, 1 mM MgSO<sub>4</sub>, 1 mM CaCl<sub>2</sub>, 5 mM KCl, 5 mM glucose, pH 7.2, 300 mOsm. RBCs were prepared by a centrifugation method consisting of a single centrifugation step at 300 × *g* to eliminate platelets and interface whitish layer, followed by several washes with the assay buffer. Occasionally, ultrapure RBC preparations were obtained via Beutler et al.'s (13) method. The latter method is said to eliminate 99% leukocytes and 90% platelets. It is based on a filtration step through a mixture of microcrystalline cellulose and  $\alpha$ -cellulose (1:1 by weight) followed by several washes by centrifugation with the assay buffer. Erythrocytes (5% hematocrit) are incubated at 37°C in different media. Under isotonic conditions, erythrocytes are incubated in buffer A. For hypotonic conditions, cells are diluted in buffer B (hypotonic) containing 32 mM HEPES, 1 mM MgSO<sub>4</sub>, 1 mM CaCl<sub>2</sub>, 5 mM glucose, pH 7.2, ~30 mOsm. For hypertonic conditions, the osmolarity of buffer A is increased up to ~900 mOsm by addition of sucrose (buffer C) and acidic conditions are achieved with buffer D containing 32 mM sodium acetate, 1 mM MgSO<sub>4</sub>, 1 mM CaCl<sub>2</sub>, 5 mM glucose, pH 5.0, ~30 mOsm. In some cases, 0.1 mM ZnCl<sub>2</sub> is added to buffer D.

### TLC

After cell incubation, lipid extraction is accomplished using a modification of a method described elsewhere (9). Briefly, to improve the chromatographic resolution of SM and prevent it from overlapping with plasmalogen and other glycerophospholipids, a 600  $\mu$ l cell suspension is incubated with 100 mM HCl at 37°C for 30 min. Afterward, alkaline hydrolysis is performed with KOH added to reach a concentration of 250 mM, followed by incubation at 70°C for 90 min. Then 3 ml chloroform/methanol (2:1, v/v) are added to the hydrolyzed cell suspension, followed by vigorous vortexing. Samples are centrifuged at 1500 × *g* for 15 min, and the lower lipid-containing chloroform phase is mixed with 4 ml water/methanol (3:2, v/v) and centrifuged under the same conditions. The lower organic phase is evaporated under nitrogen flow and the lipid film is resuspended in 80  $\mu$ l chloroform. Lipid extractions are applied to silica G60 plates and developed in chloroform/methanol/water/toluene/diethylether (60:35:8:2:1, v/v). Lipids are stained with 10% sulfuric acid (v/v) followed by heating at 110°C for 15 min. Lipid quantitation is accomplished by densitometry in a GS-800 densitometer with the Quantity One software from Bio-Rad Laboratories (Hercules, CA).

### **RP-HPLC.**

RP-HPLC measurements are performed with a Waters 2690 Alliance System and Waters 2475 fluorescence detector (Milford, MA), using a C18 reversed-phase column (Kromasil 100 C18 15 × 0.4 cm, 0.5 μm; Teknokroma, Barcelona, Spain) eluted with mixtures of water and acetonitrile containing 0.1% trifluoroacetic acid, at 1 ml/min. Empower Software from Waters Corp. (Milford, MA) is employed for data acquisition and processing.

Erythrocytes (5% hematocrit dilution) are incubated with 2 μM NBD-C<sub>6</sub>-ceramide, NBD-C<sub>6</sub>-SM, or 2 μM BODIPY-C<sub>12</sub>-SM with gentle rolling for 30 min at 4°C. The cells are then washed twice in buffer A, followed by incubation in an osmotic-shock buffer at 37°C. The reaction is terminated in ice; cells are frozen in liquid nitrogen, lyophilized, and kept at -20°C. At the time of analysis, 0.2 ml of water are added to the samples. The samples are sonicated for 30 s, vigorously mixed with 0.8 ml methanol, and centrifuged at 10,000 × g for 3 min, and the supernatant is placed in HPLC vials. Fluorescent NBD-C<sub>6</sub>-ceramide and its metabolites (λ<sub>ex</sub> = 465 nm, λ<sub>em</sub> = 530 nm) are eluted isocratically with a mobile-phase mixture of 20% water and 80% acetonitrile, whereas a linear gradient of mobile phase is used to separate BODIPY-C<sub>12</sub>-SM and its metabolites (λ<sub>ex</sub> = 505 nm, λ<sub>em</sub> = 530 nm). The elution starts from 90% acetonitrile and 10% water, and continues up to 99% acetonitrile and 1% water in 5 min. These conditions are maintained for a further 10 min. Equilibration to the starting elution conditions lasts 5 min.

### **SM quantitation by ESI-MS coupled to HPLC**

All glassware is silanated. An internal standard solution is prepared containing DLPC, DLPA, DLPS, DLPG, DLPE, and DPPI at 100 μg/ml in chloroform/methanol/water (5:5:1, v/v). Freeze-dried biological samples are resuspended in 200 μl of distilled water and extracted according to a modified Folch procedure (14). Then 200 μl of sample and 2 μg of internal standard are added to 4 ml of ice-cold acidified chloroform/methanol (2.5:1; v/v) in a glass vial. The mixture is probe-sonicated for 10 s and left at room temperature for 1 h. Samples are filtered through a 0.22 μm Durapore membrane, supplemented with 0.2 volumes 200 mM K<sub>4</sub>EDTA, and centrifuged at 800 × g for 15 min at 4°C. The organic lower phase is dried at 37°C under nitrogen and resuspended in 100 μl of chloroform/methanol/water (90:9.5:0.5, v/v). Mass spectrometry lipid analysis is carried out on an Applied Biosystems API 3000 instrument (Foster City, CA) equipped with an electrospray ionization source. Lipids are separated using a normal phase Luna silica (2) 3 μm column from Phenomenex (Torrance, CA). A gradient elution protocol (15) from 100% phase A containing chloroform/methanol/water/ethylamine (90:9.5:0.5:7; v/v) to 70% phase B chloroform/acetonitrile/methanol/water/ethylamine (30:30:35:5:10, v/v) over 20 min is used to separate SM from phosphatidylcholine (PC). PC lipids elute between 10 and 12 min, and SM lipids elute between 15 and 19 min. Phospholipids are ionized at +4kV, 300°C. SM species are determined using multiple reaction monitoring scans in which the choline group (+184 m/z) is the specific fragment for SM and PC lipids. The collision energy is +37V for SM lipids and +52V for PC lipids. Moles of SM and PC lipids are back-calculated from the internal standard and lipid peak areas by means of an in-house macro written in Excel.

### **Flickering spectroscopy**

The bending modulus of erythrocytes was measured both under isotonic conditions and in the presence of the curvature-promoting drugs CPZ and sodium deoxycholate (Na DOC) at subsolubilizing concentrations. For this purpose, 50 μl of 0.1% hematocrit diluted in isotonic buffer were loaded on a coverslip. To avoid the glass effect (16), the coverslips were previously incubated with 50 μl 0.5% casein aqueous solution for 15 min and washed abundantly with isotonic buffer. A few minutes were necessary to allow the erythrocytes to sediment. In the case of stress conditions, once an erythrocyte group was targeted, 10 μl of CPZ or Na DOC (0.8 mM final concentration) were added and gently stirred. Just after drug addition, 30-s videos were taken every minute and the thermal fluctuations of single erythrocytes were tracked by fast CCD microscopy in the phase contrast mode (Nikon TE2000-U inverted microscope with an immersion oil objective, 100×). Flickering spectroscopy, which is extensively described elsewhere (17), is well suited to measure bending properties. Briefly, the curvature fluctuations are described in Fourier series at the equatorial plane and the average amplitudes of the Fourier modes are compared with the classical Helfrich spectrum for thermal bending modes,

$$(3) P(q) = \frac{\kappa_B T}{(\sigma q^2 + \kappa q^4)},$$

obtained as a time average of the quadratic fluctuations (the time average was calculated over 500 consecutive images taken at 14 fps;  $\sigma$  is the membrane tension,  $\kappa$  is the bending stiffness, and  $q$  is the wave vector). At sufficiently large  $q$ ,  $q \approx 2/R$  ( $> \sigma/\kappa$ ), bending modes largely dominate, so when integrated over the equatorial plane, the spectrum may simply vary as  $P_x(q_x) \approx k_B T / \kappa q_x^3$ .

### **Statistics**

Unless otherwise indicated, the data are the average values of three independent measurements  $\pm 1$  SD. Student's  $t$ -test was used to assess the significance of the observed differences.

## **Results**

### **SMase activity assays.**

#### **TLC.**

SMase activity was detected in human erythrocytes after a hypotonic osmotic shock, as a decrease in SM in the first 3–6 min after the shock (Fig. 1). SM analysis by TLC and densitometry showed no variations in the SM content under isotonic conditions, whereas it decreased notably after incubation in a hypotonic medium with a specific activity of 31.8 nmoles/min  $\times$  mg ghost protein. After a 6-min incubation, the SM content decreased by 17.5% under hypotonic (hemolytic) conditions. After that time, SM levels started to increase again, suggesting the existence of mechanisms to regenerate the sphingolipid. Under isotonic conditions, the SM levels remained constant throughout the 20-min incubation.

The described neutral SMase activity could be driven by a small amount of contamination by lymphocytes. To test this possibility, we obtained a highly purified erythrocyte preparation according to Beutler et al.'s (13) method. This protocol is based on a filtration step through a mixture of microcrystalline cellulose:  $\alpha$ -cellulose (1:1) followed by several washes with the assay buffer. According to the above-mentioned protocol, 99% leukocytes and 90% platelets are eliminated from the RBC fraction. The regular centrifugation method described here is based on a centrifugation step at  $300 \times g$  to eliminate platelets and white blood cells (the interface whitish layer) and several washes with the assay buffer. Both methods yield a very similar SMase activity under hypotonic conditions (Fig. 1), confirming that the activity is indeed located in RBCs.

The initial rates measured in our system are comparable to those found in chicken RBC plasma membranes (9). However, an important difference is that in human erythrocytes, SM depletion is corrected, perhaps by de novo resynthesis, after a few minutes, whereas in chicken cells SM degradation proceeds for  $>1$  h, until most of the SM in the cell has been degraded. Thus a mechanism appears to exist in humans, but not in chickens, that helps maintain a constant SM concentration in erythrocytes.

#### **HPLC**

To assess both the variation in SM content and changes in ceramide levels, we labeled the erythrocytes with NBD- $C_6$ -SM and subjected them to hypotonic shock in buffer B. HPLC analysis of samples showed a continuous increase in NBD- $C_6$ -Cer (Fig. 2 A), which correlates with the disappearance of NBD- $C_6$ -SM (Fig. 2 B). Isotonic conditions, in which both NBD-labeled sphingolipids remained constant, were used as a negative control.

Approximately 1% of added NBD- $C_6$ -SM is degraded in the first 6 min (i.e., one order of magnitude less than the native lipid). This can be explained by a decreased affinity of the enzyme for the labeled substrate. In fact, hydrolysis was not observed for another fluorescently labeled SM (BODIPY- $C_{12}$ -SM; data not shown). Nevertheless, HPLC data showing the symmetric disappearance of NBD- $C_6$ -SM and appearance of NBD- $C_6$ -Cer (Fig. 2) qualitatively confirm the presence of a SMase activity that is detected under osmotic stress conditions but not under more-physiological (isotonic) conditions. The data in Fig. 2 also report on a continued SMase activity that remains unquenched after 20 min. This supports the idea that the SMase activity elicited by hemolysis in human RBCs is similar to that found in chicken RBCs (8, 9), although in humans a compensating biosynthetic activity occurs.

SM biosynthesis from ceramide was monitored by HPLC on human cells to which NBD-C6-Cer had been added. As shown in Fig. S1 of the Supporting Material, irrespective of isotonic and hypotonic conditions, a biosynthetic pathway exists that converts ceramide into SM. This can explain the absence of a continuing degradation and the minima in SM contents observed after 6 min (Fig. 1).

### ***HPLC-ESI-MS/MS***

Tandem HPLC-ESI-MS/MS experiments were performed to confirm the data observed by TLC and HPLC assays. In this case, we analyzed three of the most abundant phospholipids in the human erythrocyte plasma membrane (18), namely, SM, PC, and phosphatidylinositol (PI; Fig. 3). After a 6-min incubation under hypotonic conditions, 14% of the initial SM was hydrolyzed, a reduction similar to the one observed by the TLC method (17.5%). No significant differences in the PC or PI content were detected.

HPLC-ESI-MS/MS demonstrates the disappearance of individual SM species in the erythrocyte membrane after osmotic shock. The results are summarized in Table S2. Eighty percent of the sphingolipid is found in five of the 16 species detected (16:0, 18:0, 22:0, 24:0, and 24:1). Of interest, not every species is hydrolyzed at the same rate, varying from 3% hydrolyzed in 6 min (20:1) to 19.3% cleaved in the same period of time (d16:0). However, the data do not indicate a clear pattern relating lipid structure to hydrolysis rate. Although the most abundant species (16:0) is extensively cleaved, one of the less abundant (d24:0) is also highly degraded, and others (e.g., 18:1) are present in low proportions and are scarcely hydrolyzed.

### ***Mechanism of SMase activation.***

We performed a number of experiments to understand why the hypotonic conditions elicited a SMase activity. An important clue arose from studies using detergents. Detergents (or surfactants) are known to modify the activity of membrane enzymes in various ways (19, 20). As shown in Table 1, surfactants of widely different chemical structures, such as CPZ, Na DOC, and lysoPC (all at concentrations well below their critical micellar concentrations to ensure that they would interact with the membrane in the form of monomers (21)) induced SMase activity in RBCs under isotonic conditions to a similar extent as did hypotonic shock (Table 1). PLA<sub>2</sub>, which cleaves PC (among other phospholipids) to lysoPC and free fatty acids, also induced SMase activity (Table 1). One factor that is common to hypotonic shock, addition of surfactants, and enzymatic cleavage of phospholipids is the increase in membrane bending energy. In the case of hypotonic shock, bending energy is developed through an increased bilayer curvature ( $J - J_s > 0$ ), because RBCs become spherical and break down to smaller ( $\approx 2 \mu\text{m}$ ) spherical vesicles, under these conditions (22). The addition of surfactants causes the insertion of a large fraction of them predominantly into the outer lipid monolayer (23). In addition, PLA<sub>2</sub> phospholipid cleavage has the effect of increasing the bending energy because the area occupied by the free fatty acid and lysophospholipid is higher than that occupied by the original phospholipid (24, 25).

We performed a further experiment to test the bending energy hypothesis by assaying SMase activity under hypertonic conditions. In principle, RBCs should shrink under these conditions, and membrane curvature should increase as a result of decreasing cell radius. In fact, these conditions also elicit a SMase activity, as shown in Table 1. Note that under all conditions listed in Table 1, the SM levels recovered after a few minutes (data not shown), suggesting that in all cases the same phenomenon was being detected.

Thus, a number of very different, even opposing causes (hypotonic and hypertonic shocks, surfactant addition, and lipid degradation) are having a common effect, i.e., SMase activation. The only common factor we detect in this multiplicity of causes is that they all contribute to develop an accumulated membrane bending energy. Conversely, the molecular area of ceramides is smaller than that of SM (26), so that SMase has the effect of decreasing the outer monolayer area and thus the bilayer curvature and the bending energy. Consequently, SMase activity counteracts the increased bending energy, and this may explain the arrest of the enzyme activity after a few minutes. At this timescale, flip-flop motions may occur that further decrease the difference between the outer and inner monolayer areas (see Discussion).

### ***Bending modulus measurements***

The bending modulus of erythrocytes, both in the native state and in the presence of drugs, was measured by flickering spectroscopy. RBCs under isotonic conditions had a bending modulus  $\kappa \approx 1.5 \times 10^{-20} J$  (Fig. 4 A) similar to previously published values (see Evans et al. (27) and references therein).  $\kappa$  is a material parameter that depends on the lipid composition. The SM-to-ceramide conversion promoted by SMase increases the proportion of ceramides in the plasma membrane, which should become more rigid due to the presence of the newly synthesized ceramides (28, 29). In fact, when 0.8 mM CPZ, a reagent that elicited SMase activity (Table 1), was added to erythrocytes, clear changes in cell morphology were observed (Fig. 4 B). More to the point, CPZ gave rise to a 3.5-fold increase in  $\kappa$ , with a maximum 5 min after drug addition (Fig. 4 B). This corresponds to the maximum of SMase activity after CPZ addition (data not shown). The resynthesis of SM from ceramides (see Figs. 2 and 3) then decreased the value of  $\kappa$  once the maximum of SM conversion was reached. A similar increase in  $\kappa$  was observed as a consequence of SMase activity promoted by DOC (Fig. 4 C). In the same figure, data taken from Evans et al. (27) are included that correspond to hypo- and hypertonic erythrocyte membranes in which, according to our observations, SMase activity and ceramide formation might have taken place. Therefore, variations in  $\kappa$  due to the presence of newly formed ceramides in the plasma membrane constitute by themselves a different mechanism by which the bending energy can be modified.

### ***SMase activity characterization***

We further characterized the bending energy-induced SMase activity in human erythrocytes under hypo- and hypertonic conditions to study the influence of different conditions and reagents. As shown in Table S1, pH 5.0 totally abolishes SMase activity. In an important group of SMases, known as acidic SMases (10), the optimum pH is close to 5.0. Moreover, the secretory SMases (30), which are known to proceed from the same gene as acidic SMases, require  $Zn^{2+}$  for their function. However, the data in Table S1 show that  $Zn^{2+}$  failed to elicit any SMase activity at pH 5.0. Thus, these data suggest that the activity found in human RBCs may belong to the group of neutral SMases (10). In agreement with most other neutral SMases (31), SMase activity from human RBCs is activated by  $Mg^{2+}$  and  $Ca^{2+}$  (Table S1). This is at variance with the observations in chicken erythrocytes (8), where a (slight) activation by  $Mg^{2+}$  and an actual inhibition by  $Ca^{2+}$  were found.

Further proof that the SMase described above is related to the neutral SMases comes from the fact that in the presence of nSMase inhibitors such as GW4869 (32) or spiroepoxide (33), SM hydrolysis is largely or fully inhibited (Table S1). Trypsin and  $\alpha$ -chymotrypsin proteases were used under conditions in which proteins on the surface of the RBCs were hydrolyzed (34), and SMase activity was partially inhibited by trypsin and completely abolished by  $\alpha$ -chymotrypsin (Table S1). These data could suggest an association of SMase activity with a membrane protein that is accessible from the cell surface. Note that all the various agents and conditions tested had qualitatively identical effects on SMase activities elicited by hypo- and hypertonic buffers. This observation strongly reinforces the idea that both opposite factors are eliciting a single enzyme activity.

## **Discussion**

Our main observation in this study is that SMase activity may be elicited in human RBCs by a number of factors, which have in common the ability to increase the membrane bending energy.

### ***Building up the bending energy***

The spontaneous curvature model in (1), (2) recognizes that the inner and outer leaflets of a bilayer can be compositionally asymmetric. In this case, the spontaneous curvature reads:

$$(4) \quad J_S^B = \frac{(J_S^{out} - J_S^{in})}{2},$$

which is zero for a symmetric bilayer ( $J_S^{out} = J_S^{in}$ ) but finite depending on the difference between the topological curvatures of the lipids in each monolayer.

Lipid asymmetry may also produce a difference between the molecular areas of the outer and inner monolayers ( $A^{\text{out}} - A^{\text{in}} \neq 0$ ). Consequently, if the two leaflets are mechanically coupled, the bilayer takes a spontaneous curvature proportional to the net area difference (35):

$$(5) J_S^A = \frac{1}{d} \cdot \frac{A^{\text{out}} - A^{\text{in}}}{A^{\text{out}} + A^{\text{in}}},$$

where  $d$  is the monolayer thickness.

In the uncoupled case, every monolayer is free to slide past the other, thus relieving longitudinal stress upon difference area. Spontaneous curvature is not expected in this sliding case, which is characteristic of single lipid bilayers with no leaflet interdigitation. In biological membranes, due to intermonolayer lipid tail mismatch or transmembrane proteins, a certain degree of coupling is present. Therefore, if both effects are taken into account, a measurable change of the spontaneous curvature and hence of the bending energy is expected in RBCs when lipid asymmetry is induced in one of the monolayers.

Under the conditions of our experiments, RBC membrane bending is achieved through two different mechanisms: 1), changes in osmotic pressure that impose an increased curvature; or 2), increases in the outer monolayer area through insertion of surfactant molecules or cleaving of phospholipids. Note that both hypotonic shock and hypertonic shock lead ultimately to the same effect of increasing the bilayer curvature (hypotonic shock by generating smaller, spherical vesicles, and hypertonic shock by shrinking RBCs; Fig. 5).

Additionally, the accumulated energy may be also increased through increments in the bending modulus  $\kappa$  by the newly synthesized ceramide in the plasma membrane. The solid character of ceramides must increase the membrane rigidity (28, 29). This is evident in Fig. 4, where the bending modulus was increased when the SMase activity was triggered by CPZ or DOC. In this context, Evans et al. (27) measured changes in  $\kappa$  induced by hypertonic and hypotonic conditions and found that in both cases the bending modulus increased by two- to threefold in the absence of externally added drugs, probably due to the presence of the newly formed ceramide in the plasma membrane.

### ***Bending stress relaxation***

Although the change in RBC morphology was irreversible under membrane stress, the same principles may explain why SMase activity is markedly decreased after a few minutes under our conditions. First, the enzyme action itself gives rise to ceramide, whose mean molecular area is smaller than that of SM (26, 36), so that  $A^{\text{out}}$  and consequently  $J_S^B$  decrease, tending to recover the equilibrium values. Second, although surfactants and PLA<sub>2</sub> are added from the outside of the cell, thus increasing  $A^{\text{out}}$ , there will be a tendency for the lipids to flip into the internal monolayer, thus decreasing the area difference (37). In addition, SM-to-ceramide conversion is known to increase the phospholipid flip-flop rate in membranes (38, 39), in conjunction with the rapid translocation of ceramides (40), thus effectively contributing to the relaxation of bending stress due to differences in monolayer areas. Concerning the bending modulus, the observed resynthesis of SM from ceramide in the late minutes after cell stress could be the source of the bending modulus decrease observed by flickering measurements (Fig. 4 B).

DLPC is one of the amphipathic molecules that induce echinocytosis when incorporated into human RBC membranes at a final concentration of 0.2 mM (5% of the total cell phospholipid) (41), and echinocytes produced by DLPC are stable for hours. One could suppose that they should rapidly reverse to the normal form due to the bending induced by conversion of SM to ceramide in the outer monolayer. However, SM contents in human RBC accounts for ~20% of total phospholipid in the membrane (42), and our results indicate a maximum decrease of SM levels of ~15%. This means that after a 6-min induction of SMase activity, ~3% of phospholipid contents have been converted to ceramide. The higher amount of inserted amphipathic molecules as compared with the amount of produced ceramide, and the ensuing reconversion of ceramide into SM may explain why the conversion of SM into Cer cannot reverse the DLPC-induced echinocytosis effect.

### ***Proteins can sense membrane curvature***

Examples of the activation of intracellular signaling cascades in response to physical changes in the environment have been reported (43); however, the idea that membrane proteins can sense curvature is a



novel one (1). It has emerged with the identification of proteins that have membrane-binding affinities that depend on the radius of membrane curvature. ArfGAP1, a protein involved in coated-vesicle formation (44), displays a GTPase-activating activity that increases with membrane curvature. Ahyayauch et al. (45) described the increased activity of a bacterial PI-dependent phospholipase C with vesicle curvature. More recently, Urbina et al. (46) found that the SMase activity of *Clostridium perfringens*  $\alpha$ -toxin increases with curvature, whereas the phospholipase C activity of the same toxin decreases with decreasing vesicle radius. According to another report (47), the membrane lytic activity of the bacterial toxin  $\delta$ -lysin is influenced by the bending modulus. The fact that the SMase in our study could catalyze the onset of a signaling (apoptotic) cascade lends additional interest to our observation. The activation mechanism in our experiments is unclear. Assuming that the neutral SMase is localized to the inner leaflet of the membrane, membrane bending would lead to a tighter packing of this leaflet, and thus the mechanism would not simply consist of a facilitated access of the ester bonds to the active site, as one could argue if the hydrolysis took place in the outer leaflet. Reconstitution experiments with liposomes might prove useful to clarify the mechanism.

### ***Physiological implications***

The observation of a latent nSMase activity could have physiological implications. In a series of studies, Lang et al. (48, 49) related hyperosmotic shock to SMase activation, ceramide production, and apoptosis (eryptosis). However, these authors detected a maximum of ceramide production many hours after the osmotic shock, and found that SMase activation is secondary to PLA<sub>2</sub> activation and release of platelet activating factor (49). In addition, the SMase activity found by Lang et al. (48) appears to be a fumonisin-sensitive, acidic SMase, which would be very different from the one described above. In addition, it is known that nSMases are activated in the first minutes after stimulation by an extracellular signal such as TNF (50). This correlates with the activation times observed here. Also, Lacour et al. (51) described the hydrolysis of SM in HT29 human cancer cells with a maximum ceramide production after 5-min incubation with the antitumoral drug Cisplatin. Maestre et al. (52) showed the activation of nSMase activity in U937 leukemia cells after treatment with the anthracyclines doxorubicin and daunorubicin. Of interest, the SM level was decreased by ~20–22% in the first 6 min, after which the SM levels increased back to initial levels, as found in our experiments.

The mechanical stress induced in the membranes by osmotic changes is similar in nature to that caused by blood flow in the capillary system. One could expect that in both cases SM hydrolysis, an ancient stress signal (53), is triggered. It has also been suggested that ceramide might induce flip-flop lipid movements when enzymatically produced from SM by SMase (38, 39), thus bringing phosphatidylserine to the RBC outer surface and stimulating phagocytic removal of the stress-impaired cells. Moreover, membrane pores were formed in erythrocytes by hypotonic hemolysis, which gave rise to a transmembrane redistribution of phospholipids of the cell membrane (54). This scramblase activity was previously hypothesized to be a consequence of lateral mechanical stress (29, 55). In model lipid systems, the enzymatic activity of SMase in SM-containing vesicles (5% mol of total lipids) was observed to trigger drastic bilayer perturbations that provoked the formation of membrane defects, as revealed by optical microscopy and atomic force microscopy (55). It should be noted in this respect that there is no de novo ceramide synthesis in RBCs (56); thus, SM and other complex sphingolipids are the only sources of ceramide in these cells. In RBCs, the main pool of SM that is accessible to SMase is at the outer monolayer, and thus the induced mechanical stresses could be enhanced by the enzymatic SM-to-ceramide conversion. The evidence of a mechanical connection between SMase and scrambling activity suggests a strong congruence between both enzymatic systems.

### **Acknowledgements**

We thank Prof. Michael M. Kozlov from Tel Aviv University (Israel) for his help in rationalizing the physical data.

This work was supported in part by grants from the Ministerio de Educación y Ciencia (BFU 2007-62062 to F.M.G., BFU 2011-28566 to A.A., and 2005-00175/BQU to J.C. and M.E.G.), Universidad País Vasco (GIV06/42 to F.M.G.), Ministerio de Ciencia e Innovación (FIS2009-14650-C02-01 and Consolider Ingenio en Nanociencia Molecular CSD 2007-0010 to F.M.), and Comunidad de Madrid (S2005MAT-0283 and S2009MAT-1507 to F.M.). D.J.L. was a predoctoral fellow of the Basque government. I.L.-M. was supported by the Juan de la Cierva program (Ministerio de Ciencia e Innovación).

## References

1. Zimmerberg, J., and M. M. Kozlov. 2006. How proteins produce cellular membrane curvature. *Nat. Rev. Mol. Cell Biol.* 7:9–19.
2. Helfrich, W. 1973. Elastic properties of lipid bilayers: theory and possible experiments. *Z. Naturforsch. C.* 28:693–703.
3. Morales, A., H. Lee, ., J. C. Fernandez-Checa. 2007. Sphingolipids and cell death. *Apoptosis.* 12:923–939.
4. Woodcock, J. 2006. Sphingosine and ceramide signalling in apoptosis. *IUBMB Life.* 58:462–466.
5. Perry, R. J., and N. D. Ridgway. 2005. Molecular mechanisms and regulation of ceramide transport. *Biochim. Biophys. Acta.* 1734: 220–234.
6. Kolesnick, R. N., F. M. Goñi, and A. Alonso. 2000. Compartmentalization of ceramide signaling: physical foundations and biological effects. *J. Cell. Physiol.* 184:285–300.
7. Lang, K. S., S. Myssina,., T. Wieder. 2004. Involvement of ceramide in hyperosmotic shock-induced death of erythrocytes. *Cell Death Differ.* 11:231–243.
8. Hirshfeld, D., and A. Loyter. 1975. Sphingomyelinase of chicken erythrocyte membranes. *Arch. Biochem. Biophys.* 167:186–192.
9. Rousseau, A., N. Livni, and S. Gatt. 1986. Utilization of membranous lipid substrates by membranous enzymes: activation of the latent sphingomyelinase of hen erythrocyte membrane. *Arch. Biochem. Biophys.* 244:838–845.
10. Goñi, F. M., and A. Alonso. 2002. Sphingomyelinases: enzymology and membrane activity. *FEBS Lett.* 531:38–46.
11. Clarke, C. J., C. F. Snook,., Y. A. Hannun. 2006. The extended family of neutral sphingomyelinases. *Biochemistry.* 45:11247–11256.
12. Bedia, C., G. Triola, ., G. Fabria's. 2005. Analogs of the dihydroceramide desaturase inhibitor GT11 modified at the amide function: synthesis and biological activities. *Org. Biomol. Chem.* 3:3707–3712.
13. Beutler, E., C. West, and K. G. Blume. 1976. The removal of leukocytes and platelets from whole blood. *J. Lab. Clin. Med.* 88:328–333.
14. Larijani, B., D. L. Poccia, and L. C. Dickinson. 2000. Phospholipid identification and quantification of membrane vesicle subfractions by 31P-1H two-dimensional nuclear magnetic resonance. *Lipids.* 35: 1289–1297.
15. Pettitt, T. R., S. K. Dove, ., M. J. Wakelam. 2006. Analysis of intact phosphoinositides in biological samples. *J. Lipid Res.* 47:1588–1596.
16. Bessis, M. 1972. Red cell shapes. An illustrated classification and its rationale. *Nouv. Rev. Fr. Hematol.* 12:721–745.
17. Rodríguez-García, R., L. R. Arriaga, ., F. Monroy. 2009. Bimodal spectrum for the curvature fluctuations of bilayer vesicles: pure bending plus hybrid curvature-dilation modes. *Phys. Rev. Lett.* 102:128101.
18. Verkleij, A. J., R. F. Zwaal, ., L. L. van Deenen. 1973. The asymmetric distribution of phospholipids in the human red cell membrane. A combined study using phospholipases and freeze-etch electron microscopy. *Biochim. Biophys. Acta.* 323:178–193.
19. Gurtubay, J. I., J. Romay, ., J. M. Macarulla. 1980. Assay of erythrocyte-‘ghost’ proteins in the presence and absence of detergent. *Biochem. Soc. Trans.* 8:553.
20. Prado, A., J. L. Arrondo,., J. M. Macarulla. 1983. Membrane-surfactant interactions. The effect of Triton X-100 on sarcoplasmic reticulum vesicles. *Biochim. Biophys. Acta.* 733:163–171.
21. Ahyayauch, H., M. A. Requero, ., F. M. Goñi. 2002. Surfactant effects of chlorpromazine and imipramine on lipid bilayers containing sphingomyelin and cholesterol. *J. Colloid Interface Sci.* 256:284–289.
22. Montes, L. R., D. J. López, ., A. Alonso. 2008. Ceramide-enriched membrane domains in red blood cells and the mechanism of sphingomyelinase-induced hot-cold hemolysis. *Biochemistry.* 47:11222–11230.
23. Helenius, A., and K. Simons. 1975. Solubilization of membranes by detergents. *Biochim. Biophys. Acta.* 415:29–79.
24. Maggio, B. 1999. Modulation of phospholipase A2 by electrostatic fields and dipole potential of glycosphingolipids in monolayers. *J. Lipid Res.* 40:930–939.
25. Leidy, C., L. Linderoth, ., G. H. Peters. 2006. Domain-induced activation of human phospholipase A2 type IIA: local versus global lipid composition. *Biophys. J.* 90:3165–3175.
26. Hannun, Y. A., and L. M. Obeid. 2008. Principles of bioactive lipid signalling: lessons from sphingolipids. *Nat. Rev. Mol. Cell Biol.* 9:139–150.
27. Evans, J., W. Gratzler, ., J. Sleep. 2008. Fluctuations of the red blood cell membrane: relation to mechanical properties and lack of ATP dependence. *Biophys. J.* 94:4134–4144.

28. Catapano, E. R., L. R. Arriaga, ., I. Lo´pez-Montero. 2011. Solid character of membrane ceramides: a surface rheology study of their mixtures with sphingomyelin. *Biophys. J.* 101:2721–2730.
29. L´opez-Montero, I., F. Monroy, ., P. F. Devaux. 2010. Ceramide: from lateral segregation to mechanical stress. *Biochim. Biophys. Acta.* 1798:1348–1356.
30. Tabas, I. 1999. Secretory sphingomyelinase. *Chem. Phys. Lipids.* 102:123–130.
31. Clarke, C. J., and Y. A. Hannun. 2006. Neutral sphingomyelinases and nSMase2: bridging the gaps. *Biochim. Biophys. Acta.* 1758:1893–1901.
32. Marchesini, N., and Y. A. Hannun. 2004. Acid and neutral sphingomyelinases: roles and mechanisms of regulation. *Biochem. Cell Biol.* 82:27–44.
33. Arenz, C., M. Gartner, ., A. Giannis. 2001. Synthesis and biochemical investigation of scyphostatin analogues as inhibitors of neutral sphingomyelinase. *Bioorg. Med. Chem.* 9:2901–2904.
34. Cortajarena, A. L., F. M. Goñi, and H. Ostolaza. 2001. Glycophorin as a receptor for *Escherichia coli*  $\alpha$ -hemolysin in erythrocytes. *J. Biol. Chem.* 276:12513–12519.
35. Miao, L., U. Seifert, ., H. G. Do´bereiner. 1994. Budding transitions of fluid-bilayer vesicles: the effect of area-difference elasticity. *Phys. Rev. E.* 49:5389–5407.
36. Maggio, B. 2004. Favorable and unfavorable lateral interactions of ceramide, neutral glycosphingolipids and gangliosides in mixed monolayers. *Chem. Phys. Lipids.* 132:209–224.
37. Pantaler, E., D. Kamp, and C. W. Haest. 2000. Acceleration of phospholipid flip-flop in the erythrocyte membrane by detergents differing in polar head group and alkyl chain length. *Biochim. Biophys. Acta.* 1509:397–408.
38. Contreras, F. X., G. Basa˜nez, ., F. M. Goñi. 2005. Asymmetric addition of ceramides but not dihydroceramides promotes transbilayer (flip-flop) lipid motion in membranes. *Biophys. J.* 88:348–359.
39. Contreras, F. X., A. V. Villar, ., F. M. Goñi. 2003. Sphingomyelinase activity causes transbilayer lipid translocation in model and cell membranes. *J. Biol. Chem.* 278:37169–37174.
40. L´opez-Montero, I., N. Rodr´ıguez, ., P. F. Devaux. 2005. Rapid transbilayer movement of ceramides in phospholipid vesicles and in human erythrocytes. *J. Biol. Chem.* 280:25811–25819.
41. Daleke, D. L., and W. H. Huestis. 1989. Erythrocyte morphology reflects the transbilayer distribution of incorporated phospholipids. *J. Cell Biol.* 108:1375–1385.
42. Ingraham, L. M., C. P. Burns, ., R. A. Haak. 1981. Fluidity properties and liquid composition of erythrocyte membranes in Chediak-Higashi syndrome. *J. Cell Biol.* 89:510–516.
43. Rosette, C., and M. Karin. 1996. Ultraviolet light and osmotic stress: activation of the JNK cascade through multiple growth factor and cytokine receptors. *Science.* 274:1194–1197.
44. Bigay, J., P. Gounon, ., B. Antony. 2003. Lipid packing sensed by ArfGAP1 couples COPI coat disassembly to membrane bilayer curvature. *Nature.* 426:563–566.
45. Ahyayauch, H., A. V. Villar, ., F. M. Goñi. 2005. Modulation of PI-specific phospholipase C by membrane curvature and molecular order. *Biochemistry.* 44:11592–11600.
46. Urbina, P., M. Flores-D´ıaz, ., F. M. Goñi. 2011. Effects of bilayer composition and physical properties on the phospholipase C and sphingomyelinase activities of *Clostridium perfringens*  $\alpha$ -toxin. *Biochim. Biophys. Acta.* 1808:279–286.
47. Pokorny, A., E. M. Kilelee, ., P. F. Almeida. 2008. The activity of the amphipathic peptide d-lysine correlates with phospholipid acyl chain structure and bilayer elastic properties. *Biophys. J.* 95:4748–4755.
48. Lang, F., K. S. Lang, ., S. M. Huber. 2003. Cation channels, cell volume and the death of an erythrocyte. *Pflügers Arch.* 447:121–125.
49. Lang, K. S., C. Duranton, ., S. M. Huber. 2003. Cation channels trigger apoptotic death of erythrocytes. *Cell Death Differ.* 10:249–256.
50. Schu˜tze, S., T. Machleidt, ., M. Kro˜nke. 1999. Inhibition of receptor internalization by monodansylcadaverine selectively blocks p55 tumor necrosis factor receptor death domain signaling. *J. Biol. Chem.* 274:10203–10212.
51. Lacour, S., A. Hammann, ., M. T. Dimanche-Boitrel. 2004. Cisplatin-induced CD95 redistribution into membrane lipid rafts of HT29 human colon cancer cells. *Cancer Res.* 64:3593–3598.
52. Maestre, N., T. R. Tritton, ., J. P. Jaffre´zou. 2001. Cell surface-directed interaction of anthracyclines leads to cytotoxicity and nuclear factor  $\kappa$ B activation but not apoptosis signaling. *Cancer Res.* 61:2558–2561.
53. Mathias, S., L. A. Pen˜a, and R. N. Kolesnick. 1998. Signal transduction of stress via ceramide. *Biochem. J.* 335:465–480.
54. Schrier, S. L., A. Zachowski, ., P. F. Devaux. 1992. Transmembrane redistribution of phospholipids of the human red cell membrane during hypotonic hemolysis. *Biochim. Biophys. Acta.* 1105:170–176.

55. López-Montero, I., M. Veñez, and P. F. Devaux. 2007. Surface tension induced by sphingomyelin to ceramide conversion in lipid membranes. *Biochim. Biophys. Acta.* 1768:553–561.

56. Pankova-Kholmyansky, I., A. Dagan, .., E. Flescher. 2003. Ceramide mediates growth inhibition of the *Plasmodium falciparum* parasite. *Cell. Mol. Life Sci.* 60:577–587.

## Tables

**Table 1**

SMase activity elicited in human RBCs after various treatments causing increased accumulated membrane bending energy.

<b>RBC treatment</b>	<b>SMase activity (nmol SM/min × mg protein)</b>
None	2.3 ± 4.3
Hypotonic shock	31.8 ± 3.5
0.8 mM CPZ*	16.8 ± 6.2
0.8 mM Na DOC*	26.0 ± 4.1
13.2 μM lysoPC*	22.5 ± 11.2
4 U/ml PLA <sub>2</sub>	6.2 ± 0.3
8 U/ml PLA <sub>2</sub>	18.6 ± 5.7
Hypertonic shock	16.8 ± 1.3

\*Detergents used well below their critical micellar concentrations.

## Figure legends

**Figure 1.** SMase activity depending on the osmotic shock. SM from human erythrocytes was quantified after incubation in different conditions: control (isotonic, buffer A, ▲) and hypotonic (buffer B, ●, ×). RBCs were prepared according to the regular centrifugation method (●) or Beutler et al.'s (13) method for preparing ultrapure erythrocytes (×; see Materials and Methods). Mean ± SE ( $n = 9-12$ ). \*\*Significant differences between control and hypotonic conditions ( $p < 0.01$ ).

**Figure 2.** SMase activity in human RBCs labeled with NBD- $C_6$ -SM. Cells were labeled with NBD- $C_6$ -SM, incubated in hypotonic (●) or isotonic (▲) buffer, and analyzed after elution in an HPLC column. (A) Variations of NBD- $C_6$ -ceramide. (B) Variations of NBD- $C_6$ -SM. Mean ± SD ( $n = 3$ ).

**Figure 3.** Mass spectrometry analysis of different lipids in RBCs. Erythrocytes were incubated in hypotonic buffer at 37°C for 0 min (*dark bars*) and 6 min (*gray bars*). After lipid extraction, amounts of SM, PC, and PI were analyzed by mass spectrometry as described in Materials and Methods. \*Significant difference from time 0 min ( $p < 0.05$ ).

**Figure 4.** (A) Typical fluctuation spectra for different erythrocytes in the native state. The amplitudes follow a  $q_x^{-3}$  decay (*straight line*), which is characteristic of a pure bending motion. These fluctuations are well described by the Helfrich spectrum with a bending modulus of  $1.5 \times 10^{-20} J$ . (B) Changes in the erythrocyte bending modulus in the presence of 0.8 mM CPZ. Mean ± SD ( $n = 10$ ). Representative cell morphologies are shown at various times after drug addition. (C) Erythrocyte membrane bending moduli in control cells and after various treatments that elicit SMase activity: 0.8 mM CPZ, 5 min after drug addition; 0.8 mM Na DOC, 5 min after drug addition; and hyper and hypo RBCs under hyper- and hypotonic conditions, respectively (data taken from Fig. 8 b of Evans et al. (27)).

**Figure 5.** Model showing the mechanisms by which the accumulated bending energy of the membrane is increased in human RBCs. (a) Osmotic shock (hypo- or hypertonic) leads to a reduction of the cell radius, thereby increasing the spontaneous curvature of the bilayer ( $J_s^B$ ). (b) Insertion of molecules into the outer monolayer increases the area of the membrane outer leaflet and a subsequent increase in the spontaneous curvature ( $J_s^{out}$ ).

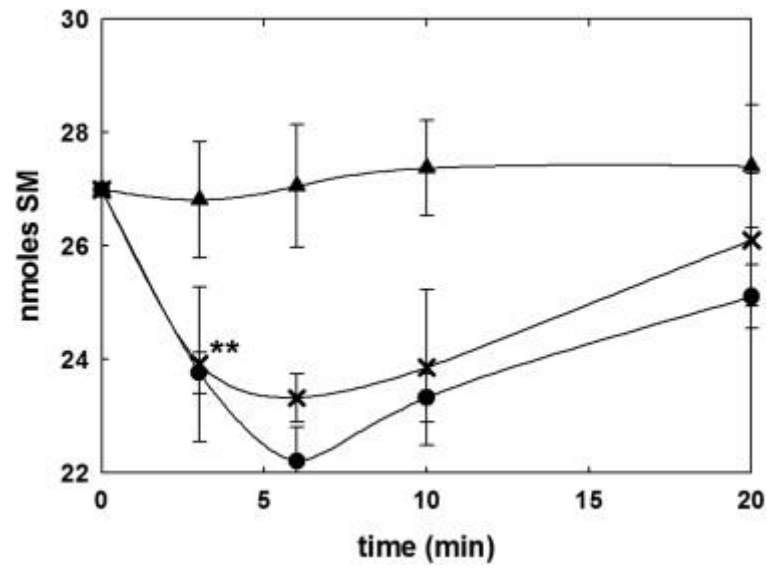


Figure 1

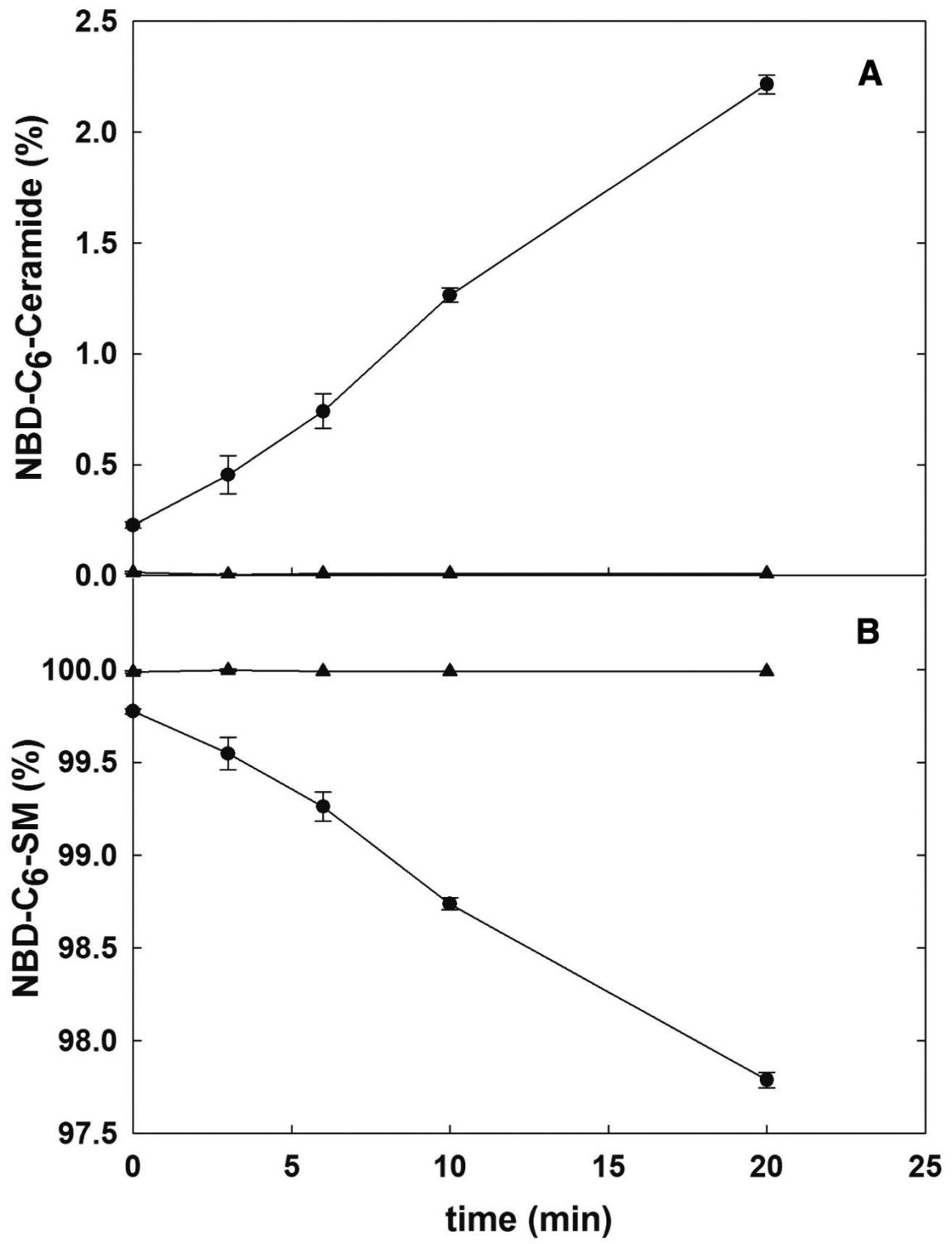
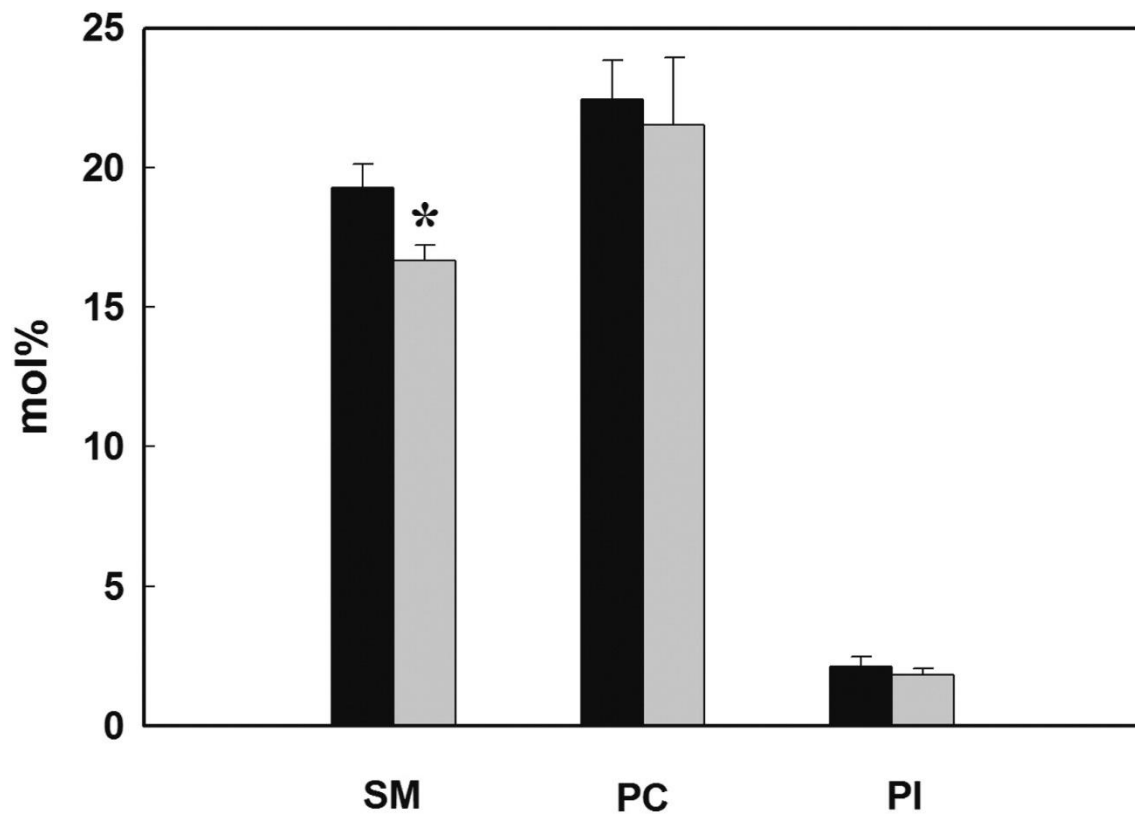


Figure 2





**Figure 3**

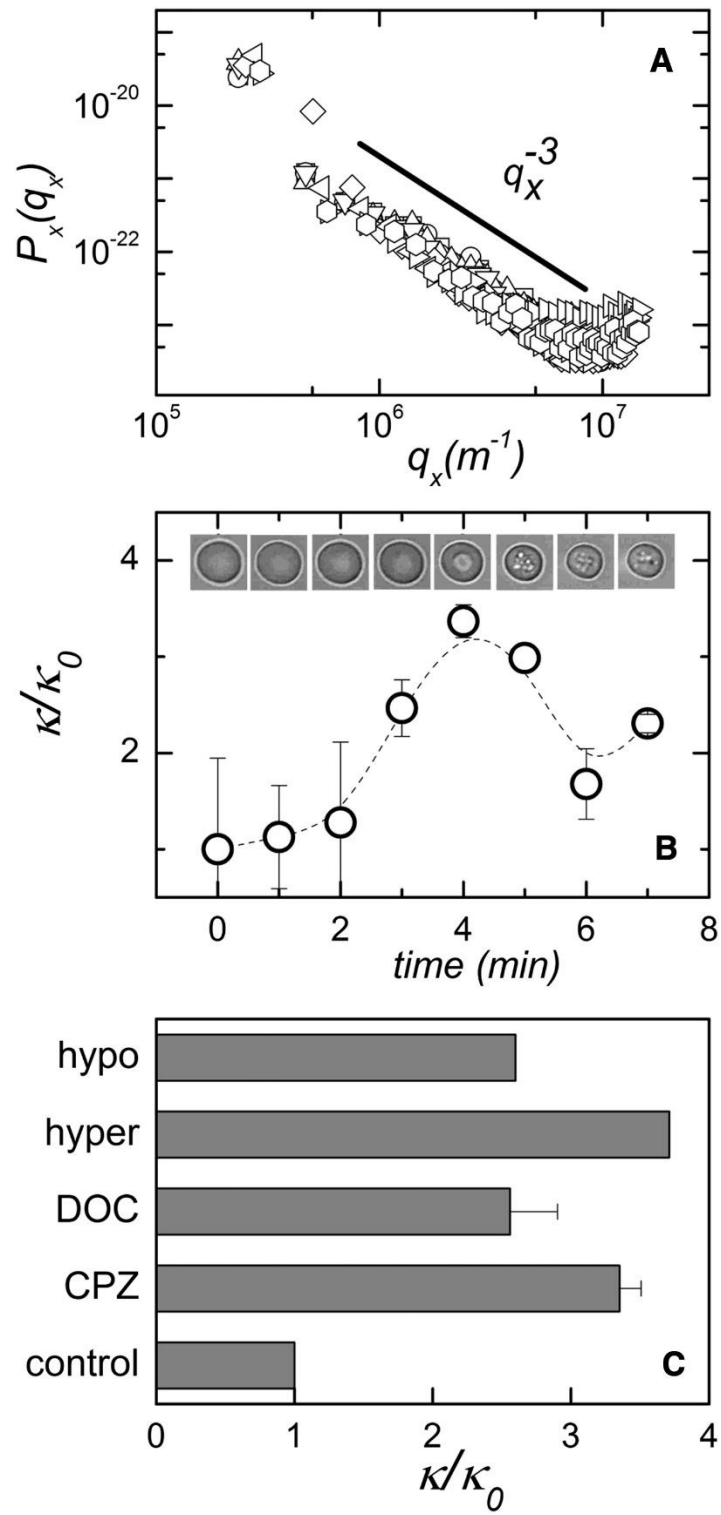


Figure 4

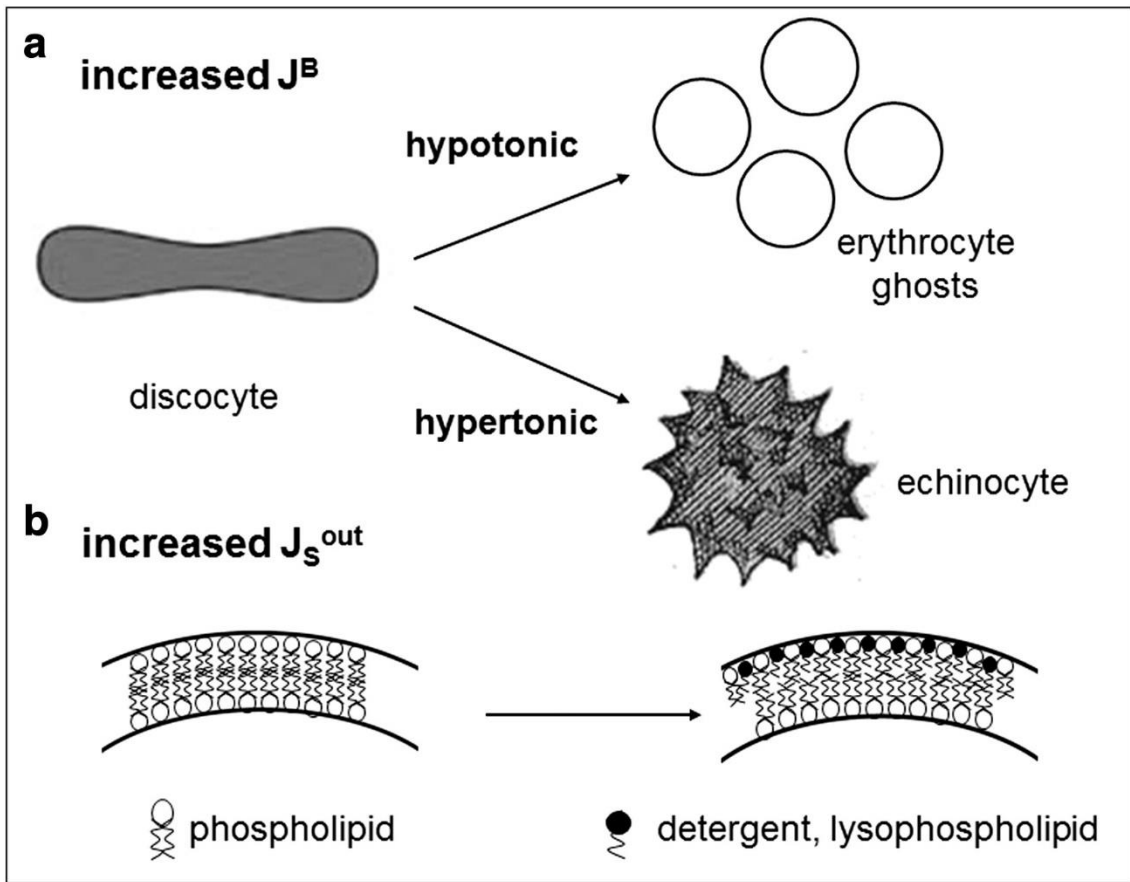


Figure 5